Detection Limit of Etched Fiber Bragg Grating Sensors

B. Nanjunda Shivananju, M. Renilkumar, Gurusiddappa R. Prashanth, Sundararajan Asokan, and Manoj M. Varma

***Abstract*—While Fiber Bragg Grating (FBG) sensors have been extensively used for temperature and strain sensing, clad etched FBGs (EFBGs) have only recently been explored for refractive index sensing. Prior literature in EFBG based refractive index sensing predominantly deals with bulk refractometry only, where the Bragg wavelength shift of the sensor as a function of the bulk refractive index of the sample can be analytically modeled, unlike the situation for adsorption of molecular thin films on the sensor surface. We used a finite element model to calculate the Bragg wavelength change as a function of thickness and refractive index of the adsorbing molecular layer and compared the model with the real-time, in-situ measurement of electrostatic layer-by-layer (LbL) assembly of weak polyelectrolytes on the silica surface of EFBGs. We then used this model to calculate the layer thickness of LbL films and found them to be in agreement with literature. Further, we used this model to arrive at a realistic estimate of the limit of detection of EFBG sensors based on nominal measurement noise levels in current FBG interrogation systems and found that sufficiently thinned EFBGs can provide a competitive platform for real-time measurement of molecular interactions while simultaneously leveraging the high multiplexing capabilities of fiber optics.**

***Index Terms*—Etched fiber Bragg grating, layer by layer assembly, limit of detection, weak polyelectrolytes.**

I. Introduction

FIBER based approaches for sensing are very attractive from the points of view of highly multiplexed detection with low cross-talk, ready availability of a large number of components from the mass produced fiber optic communication industry, compact footprint, and relatively few fabrication steps related to sensor development as the fiber itself acts as the sensor [1]. In the context of fiber sensors, the development of Fiber Bragg Gratings (FBGs) inscribed on photosensitive silica has been advantageous due to the extreme sensitivity of the resonantly reflected Bragg wavelength on the FBG parameters. Mathematically, the Bragg wavelength λ_b is related to the FBG parameters by the well known relation [2], [3].

$$\lambda_b = 2n_{eff}\Lambda \tag{1}$$

Here, n_{eff} is the effective refractive index of the optical mode propagating inside the grating inscribed optical fiber, and Λ is the grating pitch. FBG sensors have been extensively used for strain and temperature sensing where the grating pitch, Λ, is modified by these variables leading to a shift in the Bragg wavelength [4], [5]. Due to the absence of interaction of the guided optical mode with ambient environment, unmodified FBG sensors are not sensitive to surrounding refractive index (SRI). In order to make the FBGs respond to changes in SRI, one can etch the clad region as demonstrated by various groups [6]–[9] or use microfiber Bragg grating sensors [10]–[12] or by using cladding modes in long-period gratings [13], [14] which interact with surrounding medium. Etched FBGs (EFBGs) with single or few propagating modes in the core, provide a simpler output signal for spectral peak detection compared to LPGs which usually have several modes in the operating spectral band [15], [16]. Although several groups have demonstrated measurement of bulk refractive index changes, relatively few have focused on measuring surface adsorption processes using EFBGs [17], [18]. Among them Saini *et al.* have done pioneering work not only in the measurement of surface adsorption phenomena of charged polymers and DNA [19], but also proposed clever designs permitting the simultaneous measurement of refractive index, strain and temperature [20]. However, there has been no report of a carefully modeled system, where experimentally observed signals from EFBG sensors have been compared with an analytical or numerical model to quantitatively analyze the sensor data and to estimate the limits of performance based on such a validated model. We used a model system, namely, the electrostatic layer by layer (LbL) assembly of polyelectrolyte multilayers (PEMs) in conjunction with numerical finite element modeling of the optical propagation in EFBGs to quantitatively study the LbL molecular surface adsorption process using EFBGs. Such a quantitatively rigorous study has so far been lacking in the limited literature dealing with measurement of surface adsorption with EFBGs. We measured LbL of weak polyelectrolyte systems at two different pH values and showed that the assembly process is non-linear and pH dependent as reported in previous literature [21]–[24]. Using the numerical model we could rigorously verify that the non-linear growth measured by the EFBG sensors is not an artifact related to the measurement technique but an accurate reflection of the actual non-linear growth regime of these polymers. The numerical model was then used to determine the theoretical limits of

Manuscript received December 25, 2012; revised March 03, 2013; accepted May 03, 2013. Date of publication May 13, 2013; date of current version June 21, 2013. This work was supported in part by the Robert Bosch Center at the Indian Institute of Science.

B. N. Shivananju is with Department of Instrumentation and Applied Physics, Indian Institute of Science, Bangalore 560012, India.

M. Renilkumar and G. R. Prashanth are with Center for Nano Science and Engineering (CeNSE), Indian Institute of Science, Bangalore 560012, India.

S. Asokan is with Department of Instrumentation and Applied Physics, Applied Photonics Initiative, and Robert Bosch Center for Cyber Physical System, Indian Institute of Science, Bangalore 560012, India.

M. M. Varma is with Center for Nano Science and Engineering (CeNSE), and Department of Electrical Communication Engineering, Indian Institute of Science, Bangalore 560012, India.

Color versions of one or more of the figures in this paper are available online at http://ieeexplore.ieee.org.

Digital Object Identifier 10.1109/JLT.2013.2262231

detection with EFBGs with typical experimental noise figures encountered in current FBG interrogation systems. The sensitivity of EFBGs increases with decreasing fiber radius. Based on our theoretical estimates, EFBGs etched below 2 microns in diameter can achieve similar detection limits reported for currently dominant techniques for real-time monitoring of molecular interactions such as Surface Plasmon Resonance (SPR). In addition to this competitive limit of detection, fiber based sensors have an additional advantage of high multiplexing capability as mentioned before. Surpassing the limits of detection reported for SPR using EFBG sensors is limited by the challenges of maintaining mechanical robustness in ultra-thin fibers. In this context, techniques such as simultaneous measurement of strain and surface adsorption as described by Saini *et al.* [20], [25], may enable the compensation of mechanical distortions of ultra-thin fibers enabling robust measurement of molecular signals. Also, cleverly designed packaging and fluid handling systems may enable the use of high fidelity ultra-thin fiber sensors. In the rest of the paper, we describe the details of our experiment and numerical modeling along with the results and discussion.

II. Experimental Methods

A. FBG Sensor Fabrication and Measurement System

The FBG sensors were fabricated on photosensitive fiber SM1500 with core diameter 4.2 μm with refractive index of 1.4749, and cladding diameter 80 μm with refractive index 1.4440, obtained from Fibercore Inc., USA [26]. We inscribed gratings on the photosensitive core of this fiber using the phase mask technique [27] by irradiating the photosensitive core with a 3 mJ pulses with repetition rate of 200 Hz from a 248 nm KrF excimer laser beam passing through a phase mask with an approximate pitch of 1064 nm, which produced an interference pattern creating a photo-induced refractive index modulation in the core forming the fiber Bragg grating. The gratings were inscribed over a length of about 3 mm. The magnitude of the photo-induced periodic modulation of refractive index inside the core is generally of the order of 10^{-4}. The grating periodicity produced with this phase mask was approximately 532 nm giving a baseline Bragg wavelength around 1550 nm. We then etched the cladding of the FBG sensor by dipping the fiber in an aqueous solution of HF at 40% concentration. As the fiber clad is thinned, the Bragg wavelength shifts due to change in the effective refractive index of the propagating mode. This shift is a function of the fiber radius. To determine the etch stop time, we continuously monitored the Bragg wavelength from the FBG sensor being etched using an FBG interrogator system, to be described in detail later, and stopped the etching process when the shift in Bragg wavelength was 3 nm below the starting value. As the sensitivity of the FBG sensor is strongly dependent on the clad/core thickness, we used this procedure to standardize the fabrication of all our FBG sensors for the sake of uniformity. The diameter of the etched fibers was measured using a Scanning Electron Microscope (SEM) (ULTRA 55, Carl Zeiss Microscopy).

The shift of the Bragg wavelength was monitored during etching and also for the experiments described in this article using a commercial FBG interrogator system (Model SM130 from Micron Optics Inc., USA), which essentially consists of a 10 mW light source centered around 1550 nm with a 40 nm bandwidth and a high resolution optical spectrum analyzer capable of measuring the output from 4 different fibers and up to 50 multiplexed FBG sensors on each fiber. The resolution of this system is 1 pm (picometer) at a sampling rate of 1 kHz and can be improved further by averaging.

B. Polyelectrolyte LbL @ pH 5.5 and pH 7

Cationic Poly(Allylamine Hydrochloride), PAH with average mol. wt. ~15 kDa and Anionic Poly(Acrylic acid), PAA with average mol. wt. ~200 kDa were obtained from Sigma Aldrich. All polyelectrolytes were used as received without any further purification. Polyelectrolyte solutions of 10^{-2} M (based on the repeat unit molecular weight) were made from 18 MΩ DI water. The ionic strength of the polymer solutions was adjusted to 0.01 M NaCl and pH was adjusted to 5.5 or 7 with either 0.1 M HCL or 0.1 M NaOH. Polyelectrolyte deposition process involves the immersion of the EFBG into solutions of polyanions and polycations, prepared as described above in alternating sequence with a DI water rinse in between. The EFBG was bonded to the substrate using adhesive. The EFBG bonded substrate on a custom made holder was first dipped into the 80 ml polycation solution of PAH in a 100 ml beaker for 20 min, followed by dipping the EFBG in DI water for 5 min to remove loosely bound molecules. The EFBG was then immersed into the 80 ml polyanion solution of PAA in a 100 ml beaker for 20 min to adsorb a layer of PAA molecules onto the EFBG followed by the DI water rinse as described before. This process was repeated to obtain the described number of bilayers. The Bragg wavelength during the entire LbL assembly process was continuously monitored using the FBG interrogator system at a sampling rate of 1 Hz. An un-etched FBG sensor was used as a reference for any temperature fluctuation during the experiment. However, we found no evidence of temperature induced changes in our data.

C. Numerical Modeling of Surface Adsorption Sensing With EFBGs

Although an analytical model for fibers with finite clad thickness was presented by [28], it is only suitable to model bulk refractometry using EFBGs and not for modeling the effect of surface adsorption because surface adsorption creates an additional layer on top of the clad. Therefore, we created a numerical model using the RF module of the commercially available finite element solver package COMSOL. Maxwell equation was solved for the configuration shown in Fig. 2 to obtain the effective refractive index of the mode propagating in the core region. The fiber parameters were taken from manufacturers specifications as described in Section II-A. The operating wavelength was taken as 1550 nm.

The exterior boundary of the model was set as a perfect electric conductor (PEC condition). We placed the boundary sufficiently far enough ($\sim 3\times$ fiber radius) such that there was no effect of the boundary location on the calculated effective mode index. This is necessary to ensure that undesirable reflections are not corrupting the numerical analysis. To model the etching process we simply calculated the mode index n_{eff}, as a function

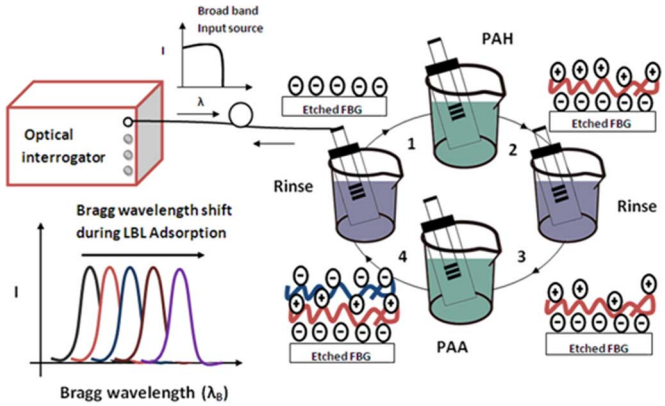

Fig. 1. Schematic of real-time monitoring of LbL assembly of polyelectrolytes using EFBG sensors.

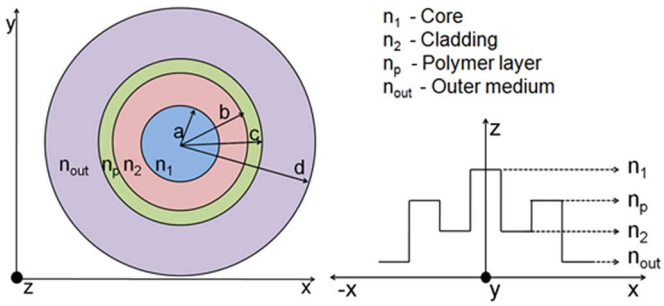

Fig. 2. Cross-sectional view of the FEM model constructed using COMSOL package to calculate the effective index change due to surface adsorption.

of the clad thickness and used (1) to convert these changes in terms of Bragg wavelength shifts. To model the molecular surface adsorption, we added another layer on top of the cladding with refractive index taken to be 1.52 based on previous literature on PAA and PAH [29]. The thickness of the adsorbed polymer layer was varied from 0 to 100 nm in increments of 10 nm. This calculation was repeated for different values of the refractive index of the outer medium, ranging from 1.33 to 1.41 in increments of 0.02. The model gave us the predicted sensitivity of the EFBG sensor as a function of the fiber radius, outer medium refractive index and other parameters. We used normalized signal changes, $\delta\lambda/\lambda$, to compare the model with experimental data.

III. Results and Discussion

We first used COMSOL to numerically calculate the mode index n_{eff} and from it, the Bragg wavelength based on (1), as a function of fiber radius.

When the clad of the FBG is etched beyond a threshold clad diameter, the effective index starts getting modulated due to the outer medium leading to a shift in the Bragg wavelength. This gives rise to a relationship between the fiber diameter and the Bragg wavelength shift arising from the etching process.

We used the model to calculate the Bragg wavelength shift expected as a function of the fiber diameter and compared this numerical data to the experimental data, which was obtained by measuring the diameter of fibers etched to a particular Bragg wavelength shift, say 2 nm, using Scanning Electron

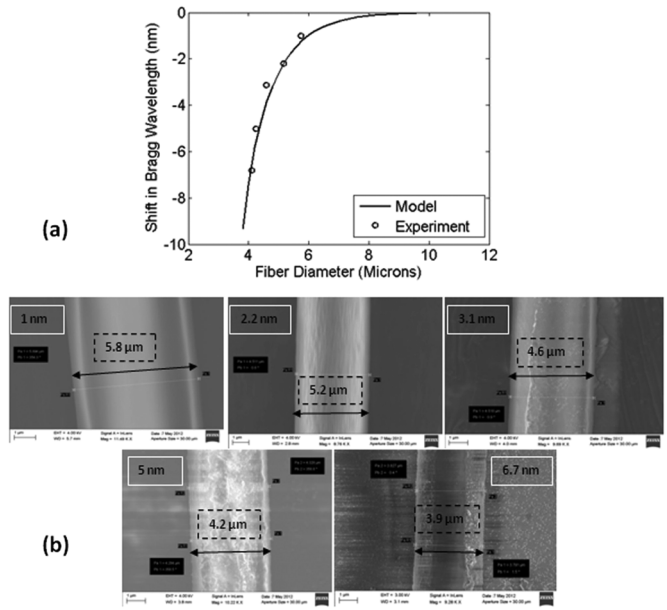

Fig. 3. Comparison of the FEM numerical model with experimentally observed Bragg wavelength shift of EFBGs as a function of fiber diameter measured using Scanning Electron Microscope (SEM).

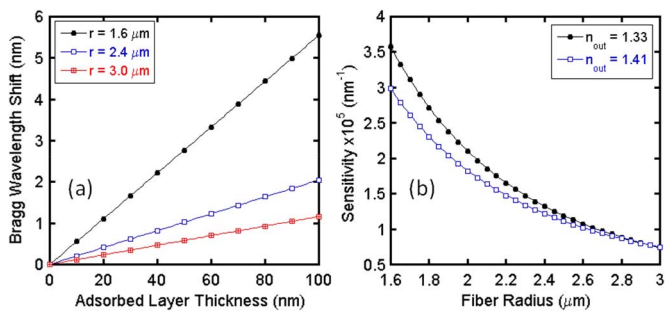

Fig. 4. a) Bragg wavelength shift due to surface adsorption calculated using the FEM model, showing a good linear behavior. Fig. 4 b) shows that sensitivity of the EFBG sensor increases faster than linearly with decreasing fiber diameter.

Microscope as described in Section II-A. As shown in Fig. 3(a), there is a good agreement between the experimental results and the numerical model, indicating the integrity of this model. In the numerical model, the refractive index of the surrounding medium was taken as 1.33 [7].

We then used the model to calculate the expected change due to surface adsorption on EFBG sensors as a function of adsorbed layer thickness. As mentioned before, we used a refractive index of 1.52 for the polyelectrolyte layer based on previous reports [29]. From Fig. 4(a), we see that there is very good linearity in the Bragg wavelength shift as a function of adsorbed layer thickness. A high degree of linearity is a desirable aspect of any sensor and in this respect EFBGs performed well. More importantly, from Fig. 4(a) and 4(b), we see that the sensitivity of the EFBG, namely the slope of the adsorption curve, increases with decreasing fiber diameter. This is because a thinner fiber effectively has more interaction with the outer medium than a thicker fiber. The slope of the adsorption curve, which we call as surface adsorption sensitivity, β_{sa}, is plotted in Fig. 4(b) as a function of fiber radius for two different outer medium indices.

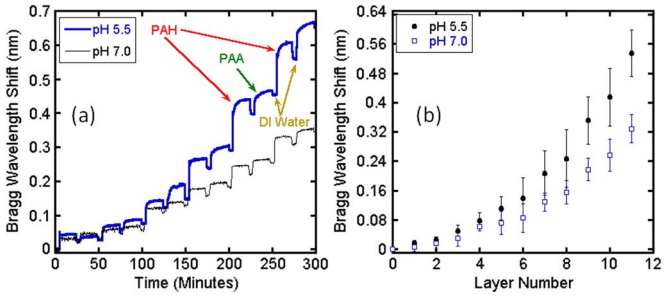

Fig. 5. LbL assembly of weak polyelectrolytes (PAH/PAA) measured in real-time with EFBG sensors. Fig. 5(a) is the real-time data and Fig. 5(b) shows the layer buildup with odd layer numbers corresponding to PAH and even layer numbers corresponding to PAA.

We see that sensitivity is slightly higher for lower medium index because of increased refractive index contrast. Most importantly, we see that the sensitivity scales faster than linearly with decreasing fiber diameter. Therefore very high sensitivities are possible by etching the FBG to smaller and smaller diameters.

The model yields a predicted value of surface adsorption sensitivity β_{sa}, which was used to convert the experimental data to a thickness value, t, using,

$$t = \frac{\left(\frac{\delta\lambda}{\lambda}\right)_{\exp}}{\beta_{sa}} \tag{2}$$

The value of β_{sa} depends on the fiber diameter and outer medium index, and can be used to normalize experiments conducted under varying conditions of these parameters.

In order to use this model to quantitatively analyze surface adsorption process, layer-by-layer (LbL) assembly of the weak polyelectrolytes PAH and PAA on the EFBG surface at pH 5.5 and pH 7 was monitored by measuring shift in the Bragg wavelength during adsorption. Fig. 5(a) shows the Bragg wavelength shift measured in real-time and 5(b) shows the layer growth as a function of number of bi-layers. The experimental data presented in Fig. 5 is the result of averaging 4 separate experiments for each pH, done on different EFBG sensors. Cationic polyelectrolyte PAH and anionic polyelectrolyte PAA were used for the polyelectrolyte multilayer assembly with a DI water rinse step between alternatively charged polymers. As a result, a multilayer thin film is built by consecutive adsorption of poly-anions and poly-cations onto the EFBG surface driven by electrostatic forces. To ensure direct comparison between the LbL depositions at pH 5.5 and pH 7, which were done on separate EFBG sensors, we ensured that both sensors were etched down to a diameter giving a 3 nm shift in the Bragg wavelength after etching, corresponding to a fiber diameter of about 4.5 μm.

From Fig. 5, we notice that pH 5.5 deposited multilayers exhibit a higher Bragg wavelength shift indicating the deposition of a thicker layer based on the model calculations shown in Fig. 4. Further we notice that the growth as a function of number of layers is not linear. Indeed these effects have been observed in the polyelectrolyte LbL literature even using non-optical measurement techniques such as Quartz Crystal Microbalance (QCM). The layer by layer assembly of weak polyelectrolytes is highly sensitive to the pH of the poly-ion dipping solutions [21]–[24]. It is known that for the weak polyelectrolyte system PAH/PAA used in this work, deposition at pH 5.5 results in thicker layers per bilayer, than the ones deposited at pH 7. This is because the polyelectrolytes are only partially charged at pH 5.5 leading to a more "loopy" conformation of polymer chains leading to thicker layers, while at pH 7, the polyelectrolytes are fully charged leading to a relatively straight chain conformation on the surface leading to thinner layers [22]. Moreover previous studies of the layer growth process using Quartz Crystal Microbalance have reported non-linear (exponential) growth for the PAH/PAA polyelectrolyte system used in our experiment [22], [23]. From these observations and results from the FEM model, we can conclude that the EFBG is indeed operating in the linear regime and the non-linear behavior observed experimentally is in fact related to the polymer assembly mechanics.

To quantitatively analyze the layer growth behavior, we converted the experimental Bragg shifts to a thickness value using (2). Previous reports of pH dependent growth of the PAH/PAA polyelectrolyte system using ellipsometry indicates an average thickness of 7 nm per bilayer for deposition at pH 5.5 and about 1 nm per bilayer for deposition at pH 7 [21]. The thicknesses extracted using our model indicate an average of 7 nm per bilayer for the pH 5.5 deposition and about 3.5 nm per bilayer for the pH 7 deposition. In this context, two important observations must be noted. Firstly, we are measuring the thicknesses of polyelectrolyte multilayers in solution while [21] reports measurements in air.

Polyelectrolyte multilayer thickness measurements in solution have never been reported before for direct comparison with existing literature. In solution, due to hydration the polymers are expected to swell to a certain extent [30]. Secondly, the molecular weight of PAH used in our experiment, namely, $\mathrm{Mw} \sim 15\ \mathrm{kDa}$ compared $\mathrm{Mw} \sim 70\ \mathrm{kDa}$ used in [21] could also significantly affect the multilayer growth dynamics. Within these uncertainties, the thicknesses extracted using our model appears reasonably within the expectations of a few nm per bilayer.

We then used two non-linear growth models to study the polyelectrolyte assembly as a function of layer numbers. Namely, an exponential [23] and a quadratic layer growth models were used to fit the thickness data as a function of layer number according to the equations,

$$t(n) = A\left(\exp(Bn) - 1\right) \tag{3a}$$

$$t(n) = Cn^2 \tag{3b}$$

In these equations, n is the layer number while A, B and C are fit parameters. The quadratic growth model has a single fit parameter while the exponential growth model has two. From Fig. 6, we see that both models fit the experimental data quite nicely. It is also interesting to observe that the exponential factor B, in (3a), is the same for LbL assembly at pH 5.5 as well as pH 7, perhaps pointing to some universal mechanism in the LbL process.

To further consolidate the integrity of our model, we performed a different experiment where 3 sensors with different fiber diameters were used to simultaneously measure the LbL assembly of PAH/PAA system deposited at pH 5.5. The 3 sen-

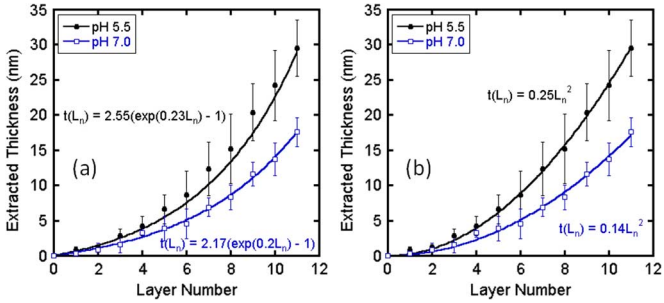

Fig. 6. Layer growth behavior of PAH/PAA LbL assembly modeled using an exponential, 6(a), and a quadratic, 6(b), growth equation as a function of layer number.

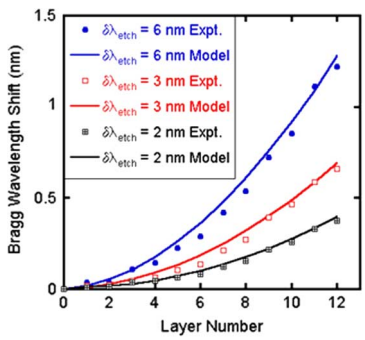

Fig. 7. Measurement of LbL assembly of PAH/PAA system at a deposition pH of 5.5 using 3 EFBG sensors with different fiber diameters, and consequently different surface adsorption sensitivities. The data can be fitted nicely using the adsorption model given by (3a) by varying only the fiber diameter as a parameter in the numerical model.

sors were fabricated by etching the FBG fibers and stopping the etching process at wavelength shifts of 2 nm, 3 nm and 6 nm respectively from their baseline Bragg wavelengths. The diameter of the fiber was then estimated using our model calculations shown in Fig. 3. As all 3 sensors are measuring the same phenomena, the thickness of the adsorbed layer would be the same on all 3 of them. However, as their sensitivities are substantially different due to the difference in diameter, we would see a family of curves from these sensors, as shown in Fig. 7. The family of curves appears solely due to the sensitivity difference between sensors and therefore we should be able to fit the data from the 3 sensors by varying only the fiber diameter, which affects the sensitivity and choosing the exponential layer growth model of (3a).

When we did this, we were able to fit the data from the 3 different sensors by varying only the fiber diameter as the parameter which conclusively demonstrated the integrity of our FEM model. Simultaneously using 3 different sensors etched to different diameters. The diameters were estimated using the FEM model based on the Bragg wavelength shift during etching and the fits were calculated using the FEM model by varying only the fiber diameter for each sensor. The good fit obtained simultaneously for all 3 sensors indicate the integrity of the FEM model.

IV. Limit of Detection (LoD) of EFBG Sensors

The primary purpose of this work was to obtain a realistic and experimentally validated estimate of the limit of detection (LoD) of the EFBG sensors for surface adsorption measurement. We wanted to benchmark the performance on EFBG sensors vis-à-vis dominant optical techniques such as Surface Plasmon Resonance (SPR) [31]. If σ is the noise level and β_{sa} is the surface adsorption sensitivity the lowest thickness detectable is with a 3σ margin, for a baseline operating wavelength of λ_0 is given by,

$$t_{\min} = \frac{3\sigma}{\lambda_0 \beta_{sa}} \tag{4}$$

The typical resolution of commercial off-the shelf FBG interrogators is about 1 pm [32], without averaging. Using this value for σ and value of β_{sa} calculated from the model, one can estimate the minimum detectable thickness for EFBGs. However, the LoD of optical detection techniques, such as SPR, is often given in terms of minimum detectable refractive index units (RIU) [31]. Therefore we need to convert the minimum thickness given by (4) into an equivalent change in refractive index, which we do in the following manner. The field outside the fiber decays exponentially with a 1/e length of d_p, as shown in Fig. 7. The effective index of the medium outside the clad region can then be written as,

$$\langle n_{eff} \rangle = \frac{\int_0^\infty n(z) \exp\left(-\frac{z}{d_p}\right) dz}{\int_0^\infty \exp\left(-\frac{z}{d_p}\right) dz} \tag{5}$$

Taking $n(z) = n_l$ from $z = 0$ to d_l, and $n(z) = n_o$ from $z = d_l$ to ∞, we obtain,

$$\langle n_{eff} \rangle = n_l \left(1 - \exp\left(-\frac{d_l}{d_p}\right)\right) + n_o \exp\left(-\frac{d_l}{d_p}\right) \tag{6}$$

Considering a small change in adsorbed layer thickness, $\delta d \ll d_p$, the equivalent effective index change due to this incremental adsorption from (6) is,

$$\delta n = \left\{ \left(\frac{n_l - n_o}{d_p}\right) \exp\left(-\frac{d_l}{d_p}\right) \right\} \delta d \tag{7}$$

Using, (7), one can convert the minimum detectable thickness, t_{min}, calculated using (4) into a minimum detectable refractive index change δn_{min}. This figure can then be compared against the limit of detection, quoted in RIU, for other optical techniques. We used the numerical model to calculate the estimated LoD for EFBGs using (4) and (7) and compared it against the LoD for SPR measurements reported in literature. There have been various SPR detection modalities that have been proposed in literature based on spectral scanning, angular scanning, phase measurements etc. These are summarized in a recent review of SPR sensing [31]. The LoD reported in [31] ranges from about 10^{-5} to about 10^{-7} for the various SPR modalities. Using the model, we calculated the LoD for EFBGs as a function of the fiber diameter. The parameters assumed for calculation was the detection of a layer with refractive index of 1.5, in a medium of refractive index 1.33, with baseline FBG wavelength of 1550 nm and other FBG parameters as reported in Section II-A. The comparison between LoDs of SPR and EFBG detection are presented in Fig. 8.

We see that the LoD decreases with decreasing fiber diameter as mentioned before. Furthermore, the LoD of EFBGs becomes

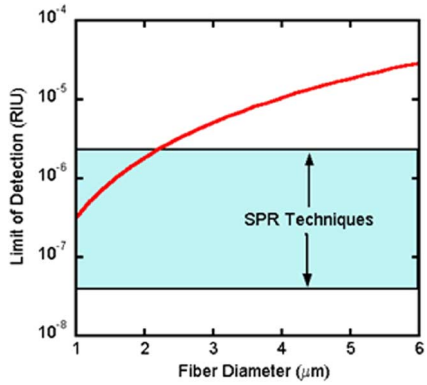

Fig. 8. Comparison of LoD of EFBGs with those reported in literature [28] for SPR. EFBGs attain competitive performance when etched below 2 microns.

competitive to SPR techniques when the fiber is etched down to below 2 microns or so. At this level, mechanical integrity of the fiber is expected to be the limiting factor in the performance of EFBG sensors. In deriving this LoD we do not consider the effect of the polymer layer itself as it is too thin relative to the fiber diameter and will also be a constant parameter for a given sensor in a practical situation.

However, we believe that with appropriate packaging and integrated fluid handling systems, it is possible to exploit the LoD scaling of EFBG fibers etched down to sub-micron levels thus providing competitive performance to SPR techniques. Additionally the inherent multiplexing abilities of fiber optical techniques are expected to be a major advantage for the creation of arrayed sensors for biomedical applications.

V. Conclusions

In summary, we used an FEM model to quantitatively analyze surface adsorption on etched FBG sensors using the widely studied phenomena of electrostatic layer by layer assembly of polyelectrolyte molecules. We found the results of the numerical model to be in reasonable agreement with previous studies of polyelectrolyte assembly. We used this numerical model to obtain a realistic estimate of EFBG limit of detection as a function of fiber radius and observed that EFBGs can offer competitive performance to currently dominant optical techniques such as SPR when the fiber is etched down to 2 microns or below. In order to take advantage of the LoD scaling observed with fiber diameter, design of novel methods for packaging the thinned EFBG sensor to provide good mechanical robustness is essential.

References

[1] B. Lee, "Review of the present status of optical fiber sensors," *Opt. Fiber Technol.*, vol. 9, no. 2, pp. 57–79, Apr. 2003.

[2] A. D. Kersey, M. A. Davis, H. J. Patrick, M. LeBlanc, K. P. Koo, C. G. Askins, M. A. Putnam, and E. Friebele, "Fiber grating sensors," *J. Lightw. Technol.*, vol. 15, no. 8, pp. 1442–1463, Aug. 1997.

[3] A. Othonos, "Fiber Bragg gratings," *Rev. Sci. Instrum..*, vol. 68, no. 12, pp. 4309–4341, Dec. 1997.

[4] S. W. James, M. L. Dockney, and R. P. Tatam, "Simultaneous independent temperature and strain measurement using in-fibre Bragg grating sensors," *Electron. Lett.*, vol. 32, no. 12, pp. 1133–1134, Jun. 1996.

[5] X. Shu, K. Chisholm, I. Felmeri, K. Sugden, A. Gillooly, L. Zhang, and I. Bennion, "Highly sensitive transverse load sensing with reversible sampled fiber Bragg gratings," *Appl. Phys. Lett.*, vol. 83, no. 15, pp. 3003–3005, Oct. 2003.

[6] D. A. Pereira and J. L. Santos, "Fiber Bragg grating sensing system for simultaneous measurement of salinity and temperature," *Opt. Eng.*, vol. 43, no. 2, pp. 299–304, Feb. 2004.

[7] A. N. Chryssis, S. M. Lee, S. B. Lee, S. S. Saini, and M. Dagenais, "Highly sensitivity evanescent field fiber Bragg grating sensor," *IEEE Photonic. Technol. Lett.*, vol. 17, no. 6, pp. 1253–1255, Jun. 2005.

[8] W. Liang, Y. Huang, Y. Xu, R. K. Lee, and A. Yariv, "Highly sensitive fiber Bragg grating refractive index sensors," *Appl. Phys. Lett.*, vol. 86, no. 15, p. 151122, Apr. 2005.

[9] A. Iadicicco, A. Cusano, S. Campopiano, A. Cutolo, and M. Giordano, "Thinned fiber Bragg gratings as refractive index sensors," *IEEE Sens. J.*, vol. 5, no. 6, pp. 1288–1295, Dec. 2005.

[10] J. L. Kou, M. Ding, J. Feng, Y. Q. Lu, F. Xu, and G. Brambilla, "Microfiber-based Bragg gratings for sensing applications: A review," *Sensors*, vol. 12, pp. 8861–8876, 2012.

[11] Y. Ran, Y. N. Tan, L. P. Sun, S. Gao, J. Li, L. Jin, and B. O. Guan, "193 nm excimer laser inscribed Bragg gratings in microfibers for refractive index sensing," *Opt. Exp.*, vol. 19, no. 19, pp. 18577–18583, Sept. 2011.

[12] G. Wang, P. P. Shum, H. P. HO, X. Yu, D. J. J. Hu, Y. Cui, L. Tong, and C. Lin, "Modeling and analysis of localized biosensing and index sensing by introducing effective phase shift in microfiber Bragg grating (μFBG)," *Opt. Exp.*, vol. 19, no. 9, pp. 8930–8938, Apr. 2011.

[13] S. W. James and R. P. Tatam, "Optical fibre long-period grating sensors: Characteristics and application," *Meas. Sci. Technol.*, vol. 14, pp. 49–61, 2003.

[14] A. Iadicicco, S. Campopiano, M. Giordano, and A. Cusano, "Spectral behavior in thinned long period gratings: Effects of fiber diameter on refractive index sensitivity," *Appl. Opt.*, vol. 46, no. 28, pp. 6945–6952, Oct. 2007.

[15] N. Chen, B. Yun, and Y. Cui, "Cladding mode resonances of etch-eroded fiber Bragg grating for ambient refractive index sensing," *Appl. Phys. Lett.*, vol. 88, p. 133902, Mar. 2006.

[16] N. Chen, B. Yun, Y. Wang, and Y. Cui, "Theoretical and experimental study on etched fiber Bragg grating cladding mode resonances for ambient refractive index sensing," *J. Opt. Soc. Amer. B.*, vol. 24, no. 3, pp. 439–445, Mar. 2007.

[17] G. Ryu, M. Dagenais, M. T. Hurley, and P. Deshong, "High specificity binding of lectins to carbohydrate-functionalized fiber Bragg gratings: A new model for biosensing applications," *IEEE J. Quantum Electron.*, vol. 16, no. 3, pp. 647–653, 2010.

[18] S. S. Saini, C. Stanford, S. M. Lee, J. Park, P. Deshong, W. E. Bentley, and M. Dagenais, "Monolayer detection of Biochemical agents using etched-core fiber Bragg grating sensors," *IEEE Photon. Technol. Lett.*, vol. 19, no. 18, pp. 1341–1343, Sep. 2007.

[19] A. N. Chryssis, S. S. Saini, S. M. Lee, H. Yi, W. E. Bentley, and M. Dagenais, "Detecting hybridization of DNA by highly sensitive evanescent field etched core fiber Bragg grating sensors," *IEEE J. Quantum Electron.*, vol. 11, no. 4, pp. 864–872, 2005.

[20] S. M. Lee, S. S. Saini, and M. Y. Jeong, "Simultaneous measurement of refractive index, temperature, and strain using etched-core fiber Bragg grating sensors," *IEEE Photonic. Technol. Lett.*, vol. 22, no. 19, pp. 1431–1433, Oct. 2010.

[21] J. Choi and M. F. Rubner, "Influence of the degree of ionization on weak polyelectrolyte multilayer assembly," *Macromolecules*, vol. 38, no. 1, pp. 116–124, Dec. 2005.

[22] T. Yamada and S. Shiratori, "In situ observation of the initial absorption process of Layer-by-Layer sequential adsorbed polyelectrolyte film using an AFM," *Electr. Eng. Jpn.*, vol. 141, no. 2, pp. 1–7, 2002.

[23] P. Bieker and M. Schonhoff, "Linear and exponential growth regimes of multilayers of weak polyelectrolytes in dependence on pH," *Macromolecules*, vol. 43, no. 11, pp. 5052–5059, May 2010.

[24] S. S. Shiratori and M. F. Rubner, "pH dependent thickness behavior of sequentially adsorbed layers of weak polyelecytolytes," *Mactomolecules*, vol. 33, no. 11, pp. 4213–4219, Apr. 2000.

[25] S. M. Lee, M. Y. Jeong, and S. S. Saini, "Etched-core fiber Bragg grating sensors integrated with microfluidic channels," *J. Lightw. Technol.*, vol. 30, no. 8, pp. 1025–1031, Apr. 2012.

[26] FIBERCORE,SM-Series-Single-Mode-Fibers [Online]. Available: http://www.fibercore.com/LinkClick.aspx?fileticket=BLXitwhVFOQ%3D&tabid=68&mid=621

[27] K. O. Hill, B. Malo, F. Bilodeau, D. C. Johnson, and J. Albert, "Bragg grating fabricated in monomode photosensitive optical fiber by UV exposure through a phase mask," *Appl. Phys. Lett.*, vol. 62, no. 10, pp. 1035–1037, Mar. 1993.
[28] M. Monerie, "Propagation in doubly clad single-mode fibers," *IEEE J. Quantum Electron.*, vol. 18, no. 4, pp. 535–542, Apr. 1982.
[29] S. Fujita and S. Shiratori, "The optical properties of ultra-thin films fabricated by layer-by-layer absorption process depending on dipping time," *Thin Solid Films*, vol. 499, pp. 54–60, Mar. 2006.
[30] G. Dechner and J. Schlenoff, *Multilayer Thin Films*. Weinheim: Wiley, 2002.
[31] A. Shalabney and I. Abdulhalim, "Sensitivity-enhancement methods for surface Plasmon sensors," *Laser Photonics Rev.*, vol. 5, no. 4, pp. 571–606, Mar. 2011.
[32] Optical-Sensing-Interrogator/SM130 [Online]. Available: http://www.micronoptics.com/uploads/library/documents/Datasheets/Micron%20Optics%20sm130.pdf

B. Nanjunda Shivananju was born India, in 1984. He received the B. E. degree from Bangalore Institute of Technology, Bangalore, India. He is currently pursuing PhD degree in Instrumentation and Applied Physics, Indian Institute of Science, Bangalore, India. His thesis research was focused on Bio-Chemical sensing by using Fiber Bragg Grating sensor.

M. Renilkumar received the B.Sc. degree from Kannur University, Kerala, India, in 2002, and the M.Sc. degree from Bharathidasan University, Tiruchirappalli, India, in 2005, both in physics. He obtained a Ph.D. in Physics from Anna University, Chennai, India, in 2012. He is currently a Postdoctoral fellow at Center for Nano Science and Engineering, Indian Institute of Science, Bangalore, India. His research interests cover integrated silicon photonics, MEMS, and development of micro/nanodevices based on photonic band gap for fiber optics and biomedical sensing applications.

Gurusiddappa R. Prashanth is a doctoral student in the Department of Electrical Communication Engineering at the Indian Institute of Science, Bangalore. He is working on developing optical applications using layer by layer assembly of polyelectrolytes.

Sundararajan Asokan obtained his Ph.D. from Indian Institute of Science, Bangalore in the Division of Physical and Mathematical Sciences. He is currently a Professor at the Department of Instrumentation and Applied Physics, and Applied Photonics Initiative, and Chairman for Robert Bosch Center for Cyber Physical Systems, Indian Institute of Science, Bangalore. His interests span a variety of topics related to Fiber Bragg Grating Sensors and Phase Change Memory using Chalcogenide glasses.

Manoj M. Varma obtained his Ph.D. from Purdue University in 2005. He is currently an Assistant Professor at the Center for Nano Science and Engineering (CeNSE), Indian Institute of Science, Bangalore. His interests span a variety of topics related to label-free bio-molecular sensing.